DOI: 10.1002/chem.200903439

Dipyrenylcalix[4]arene—A Fluorescence-Based Chemosensor for Trinitroaromatic Explosives

Young Hoon Lee,[a] Hongguang Liu,[b] Jin Yong Lee,*[b] Sang Hoon Kim,[a] Sung Kuk Kim,[c] Jonathan L. Sessler,[c] Yang Kim,[d] and Jong Seung Kim*[a]

Abstract: A new chemosensor-based approach to the detection of nitroaromatics is described. It involves the analyte-induced quenching of excimer emission of a dipyrenyl calix[4]arene (**L**). The chemical and photophysical properties of the complexes formed between **L** and mono-, di-, and trinitrobenzene, and di- and trinitrotoluene were studied in acetonitrile and chloroform by using ^{1}H NMR, UV/Vis, and fluorescence spectroscopy. Fluorescence spectroscopy revealed that the trinitroaromatics engendered the largest response among the various substrates tested, with the sensitivity for these analytes being correspondingly high. Quantitative analysis of the fluorescence titration profile generated from the titration of **L** with TNT provided evidence that this particular functionalized calix[4]arene receptor allows for the detection of TNT down to the low ppb level in CH_3CN. A single-crystal X-ray diffraction analysis revealed that in the solid state the complex **L**·TNT consists of a supramolecular crystalline polymeric structure, the formation of which appears to be driven by intermolecular π–π interactions between two pyrene units and a TNT molecule held at a distance of 3.2–3.6 Å, as well as by intra- and intermolecular hydrogen-bonds among the amide linkages. Nevertheless, the changes in the ^{1}H NMR, UV/Vis, and fluorescence spectrum, including sharp color changes, are ascribed to a charge-transfer interaction arising from complementary π–π overlap between the pyrene subunits and the bound trinitroaromatic substrates. A number of ab initio calculations were also carried out and, considered in concert, they provide further support for the proposed charge-transfer interactions, particularly in the case of **L**·TNT.

Keywords: calixarenes · density functional calculations · fluorescence · nitroaromatics · sensors

Introduction

Quick and reliable sensors for the detection of high explosives are in demand for the protection of lives and property, environmental remediation, minefield restoration, forensic analysis, and national security.[1,2] Trinitroaromatics are well-known high explosives, but are also recognized as environmental contaminants. For example, the soil and ground water of war zone and military facilities can contain toxic levels of these compounds and their degradation products.[3]

Concentrations of trinitroaromatics in ground water and soil sites near an unexploded explosive can reach levels exceeding 500 ppb and between 1000–5000 ppm, respectively.[4] TNT, one of the widely used trinitroaromatic explosives, is poisonous and can cause skin irritation, anemia, and abnormal liver functions when it is ingested or inhaled.[4] Moreover, TNT adversely affects male fertility and is now regarded as a possible human carcinogen.[4] Therefore, the US Environmental Protection Agency (EPA) has set a limit of 2 ppb for TNT in drinking water.[5]

[a] Dr. Y. H. Lee, S. H. Kim, Prof. J. S. Kim
Department of Chemistry, Korea University
Seoul 136-701 (Republic of Korea)
Fax: (+82) 2-3290-3121
E-mail: jongskim@korea.ac.kr

[b] H. Liu, Prof. J. Y. Lee
Department of Chemistry, Sungkyunkwan University
Suwon 440-746 (Republic of Korea)
E-mail: jinylee@skku.edu

[c] S. K. Kim, Prof. J. L. Sessler
Department of Chemistry and Biochemistry
The University of Texas at Austin, Austin
Texas 78712-0165 (USA)

[d] Prof. Y. Kim
Department of Chemistry & Advanced Materials
Kosin University, Busan 606-701 (Republic of Korea)

Supporting information for this article is available on the WWW under http://dx.doi.org/10.1002/chem.200903439.

Currently, a range of instrumental techniques is available for the purpose of explosives detection; these include GC-MS, surface-enhanced Raman spectroscopy, X-ray imaging, nuclear quadrupole resonance, thermal and fast neutron analysis, ion mobility spectrometry, and various spectroscopic methods.[6] These analytes have also been analyzed by electrochemical methods due to their inherent redox activity.[7] While highly efficient and in many instances remarkably sensitive, these methods, as a rule, rely on expensive instrumentation and are generally plagued by a lack of portability. There thus remains a need for detection strategies that are cheap and easy to use. One particularly promising approach would involve the use of a fluorescence-based chemosensor. Fluorescence-based detection offers several advantages over other analytical methods with respect to high sensitivity, specificity, and real-time monitoring with fast response times.[8] To date, considerable effort has been devoted to the development of fluorescence-sensing materials to detect nitroaromatics. For example, fluorescence-functionalized polymers;[9] luminescent polymer nanoparticles, such as siloles[6,10] and pentiptycene;[11] and fluorescent silicon nanoparticles,[12] have been synthesized to validate the detection of trinitroaromatics by the fluorescence spectroscopy. Nevertheless, stand-alone single-molecule systems that may be used for the detection of nitroaromatics through fluorescence-based approaches remain rare.[13] We recently reported several colorimetric systems for the detection of these species.[14] However, because the method of analysis relied on changes in color, the sensitivity of these systems remains low compared to what might potentially be achievable by using a fluorescence-based approach.

There are several mechanisms that can be exploited to impart large, analyte-induced changes in the fluorescence properties of a chemosensor upon interaction with a targeted guest molecule (e.g., nitroaromatic analyte). These include photoinduced electron transfer (PET), fluorescence (Förster) resonance energy transfer (FRET), excimer/exciplex formation or extinction, and photoinduced charge transfer (PCT).[15] Appropriately constructed dimeric pyrenes are a particularly interesting set of fluorophores in this regard; they are characterized by an interesting fluorescence relationship between the monomer and excimer emission, resulting from a strong π–π interaction between two pyrenes, that can be modulated upon interaction with a substrate.[16] In fact, ratiometry involving the excimer/monomer of multipyrenyl groups has been exploited recently as an effective sensing tools for various guest molecules.[17,18] However, fluorescence-sensing systems based on pyrenyl derivatives for organic nitro species are not well developed.[3,19] We have thus extended our recent work on luminescent pyreneamide-appended calix[4]arene derivatives to the problem of trinitroaromatics recognition and wish to report here that this approach provides an effective and sensitive means of detecting such classic nitroaromatic explosives as TNT (=2,4,6-trinitrotoluene) and TNB (=1,3,5-trinitrobenzene). In particular, we provide evidence for the proposed supramolecular interaction between calix[4]arene **L** and TNT obtained by X-ray crystallography. We also show that this analyte, as well as certain other highly nitrated electron-deficient aromatics, leads to an effective quenching of the pyrene fluorescence of **L**, with a sensitivity that allows for detection at the low ppb level in acetonitrile.

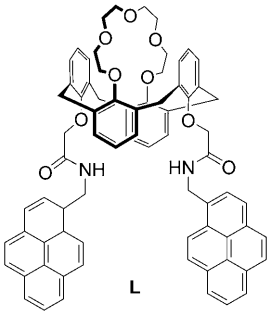

L

Results and Discussion

The bispyrene-appended 1,3-alternate calix[4]arene receptor (**L**) was prepared by using a modification of our previously reported synthetic procedures.[17b] As in our earlier studies, the bridging polyether plays a key structural role, serving to lock the conformation of the calix[4]arene core and thus orient the two pyrene substituents to the same side of the receptor ensemble.

Compound **L** displays both monomer ($\lambda_{em}=375$ nm) and excimer ($\lambda_{em}=470$ nm) emissions when irradiated at 343 nm in CH_3CN, as illustrated in Figure 1 and Figure S1 in the Supporting Information. These emission features (both the monomer and excimer bands) are quenched upon addition of TNT (Figure 1) or TNB (Figure S1 in the Supporting Information). Similar quenching is also observed in $CHCl_3$ (Figure S3 in the Supporting Information) The analyte-induced reduction in emission intensity is ascribed to the formation of charge-transfer complexes between the electron donor (pyrene) and the electron acceptor (quencher).[19e] Such a mechanistic rationale is consistent with previous re-

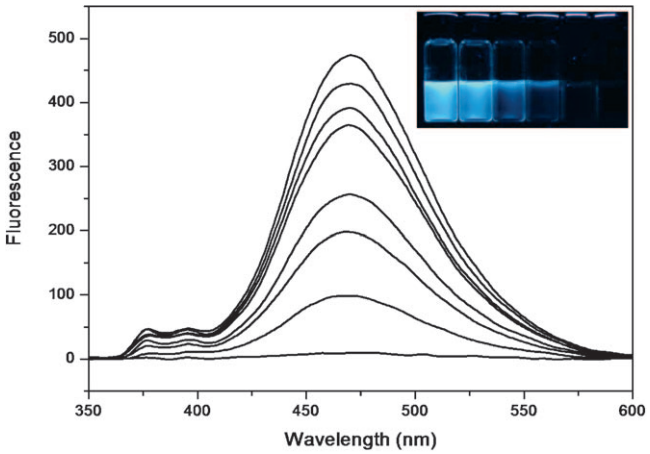

Figure 1. Fluorescence quenching and visual changes observed upon subjecting a 20 μM solution of **L** in CH_3CN to titration with increasing quantities of TNT in this same solvent (from top to bottom and from left to right in the insert: 0, 1, 5, 10, 30, 50, 100, 300 equiv) with excitation at $\lambda_{ex}=343$ nm.

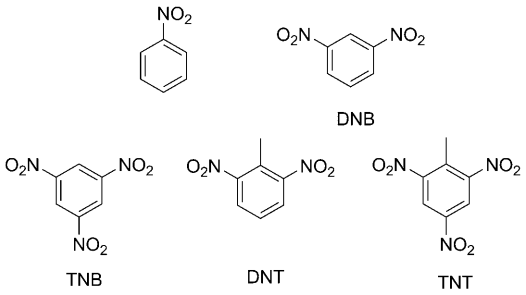

ports in which it was suggested that thermodynamically favorable exciplex formation between a fluorophore and a quencher involves strong coupling of the respective π electrons, which in turn leads to deactivation of the fluorophore excited singlet state.[20]

We also investigated the effect that other aromatic compounds, specifically those shown above, had on the fluorescence features of **L** as recorded in CH_3CN with $\lambda_{ex}=343$ nm. The results of these studies are summarized in Figure 2. As

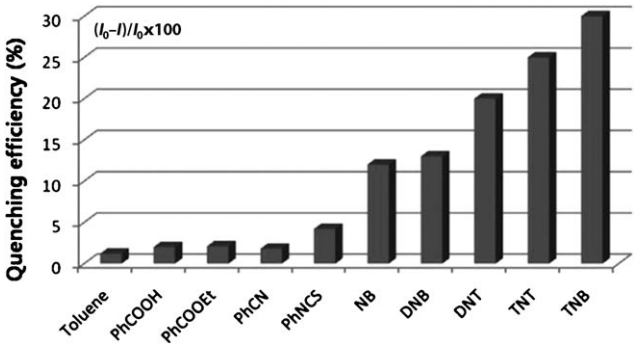

Figure 2. Reduction in fluorescence intensity (plotted as quenching efficiency) seen upon the addition of guest molecules (L/guest = 1:10 in CH_3CN; excitation at 343 nm, analysis at $\lambda_{ex}=470$ nm). NB = nitrobenzene, DNB = 1,3-dinitrobenzene, DNT = 2,6-dinitrotoluene, TNB = 1,3,5-trinitrobenzene, and TNT = 2,4,6-trinitrotoluene.

can be seen from an inspection of this figure, the most electron-deficient aromatic substrates engendered the greatest quenching. On the other hand, electron-neutral and electron-rich aromatic species, such as toluene, benzoic acid, ethyl benzoate, benzonitrile, and phenylthiocyanate, induced little or no quenching. Such a finding is fully consistent with the proposed mechanism, in which the targeted nitroaromatic analyte acts as a fluorescence quencher as the result of a charge-transfer event. Indeed, the greater the number of electron-withdrawing nitro ($-NO_2$) groups present on the benzene or toluene core, the more extensive the degree of fluorescence quenching; this is as would be expected under a scenario in which the charge transfer between the pyrene subunits and the electron acceptors becomes enhanced.

To evaluate the sensitivity of **L** toward TNT, a fluorescence titration was performed by using low concentrations of both the receptor and the analyte in CH_3CN (Figure S2 in the Supporting Information). This analysis revealed that this particular chemosensor enables an instrument-discernible response down to the ≈1.1 ppb level in CH_3CN. While the limitations of this solvent environment must be stressed, it is worth noting that this level of sensitivity falls below the permissible limit of 2.0 ppb for TNT in drinking water established by the US EPA.[5]

To gain insight into the nature of the interaction between the calixarene-based sensor **L** and TNT, a single-crystal X-ray diffraction analysis was carried out on an orange single crystal of **L**·TNT obtained by slow diffusion of diethyl ether into a solution of **L**·TNT in dichloromethane. This solid-state structure confirms that the calix[4]arene moiety **L** is in 1,3-alternate conformation (Figure 3). It also reveals that

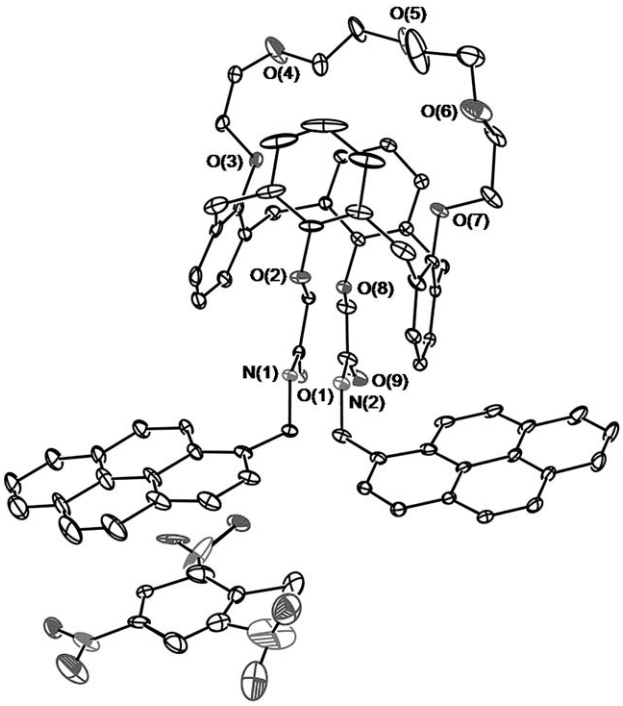

Figure 3. Crystal structure of complex **L**·TNT. The displacement ellipsoids have been drawn at the 15% probability level. Hydrogen atoms and solvent molecules have been omitted for clarity.

the two amide groups are involved in interamolecular hydrogen-bonding (N(2)–H(2)···O(1) = 2.027 Å), as well as in intermolecular hydrogen-bonding interactions involving a neighboring amide (N(1)–H(1)···O(9) = 2.161 Å). These last interactions are presumably responsible for the formation of a supramolecular linear polymer network, as revealed in a packing diagram of the structure.

Interestingly, the X-ray structure also revealed that the two pyrene substituents present in **L** are splayed outwards (i.e., oriented in an equatorial conformation relative to the rest of the receptor molecule) and interact with the co-bound TNT molecule by what appears to be a donor acceptor interaction (Figure 4). While this interaction orients the TNT parallel to a pyrene subunit at a distance of 3.2–3.6 Å

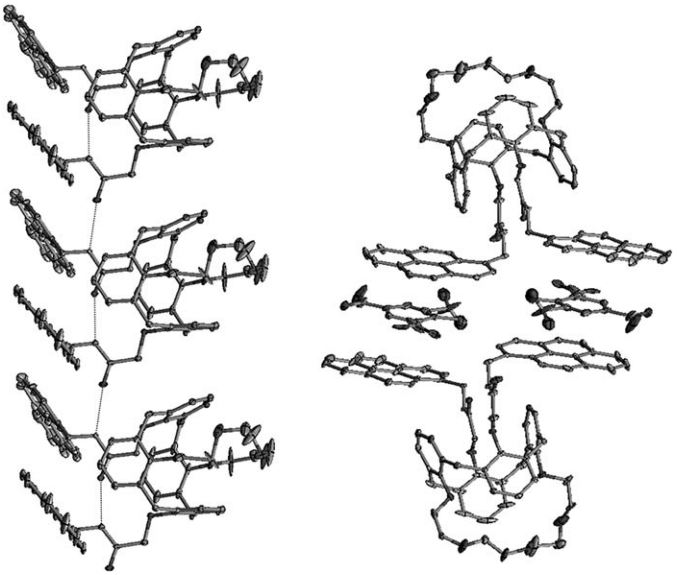

Figure 4. Different views of the solid state structure of **L**·TNT complex presented in Figure 3. Left: polymeric structure stabilized by hydrogen bonding. Right: intermolecular interaction between two neighboring pyrene moieties and TNT.

relative to the π surfaces, the binding takes place outside of the putative cleft that would have been formed were the pyrenes to be oriented in a parallel or axial fashion relative to the calixarene skeleton. Nevertheless, this structure serves to confirm that the supramolecular donor–acceptor interactions invoked to explain the observed fluorescence quenching are chemically reasonable. In fact, to the best of our knowledge, the crystal structure given in Figure 4 is the first to illustrate the existence of such a binding motif involving pyrene and TNT in the solid state.

Efforts were also made to determine whether **L** could be used as a naked-eye detectible colorimetric chemosensor for nitroaromatic compounds at higher concentrations of receptor and substrate. Because the solubility of **L** is rather poor in CH_3CN, in contrast to the fluorescence-based analyses described above (in which both CH_3CN and $CHCl_3$ were used; vide supra), these studies were only carried out in chloroform. As shown in Figure 5 (top), solutions of **L** in chloroform, when treated with the more electron-deficient trinitroaromatics of the present study (i.e., TNT or TNB; colorless species), were found to undergo a marked and easily visible change in color from pale yellow to reddish orange. This change in color is instantaneous on the human timescale and is characterized by corresponding changes in the UV/Vis absorption spectrum (cf. Figure S4 and S5 in the Supporting Information) and is fully reflected in the ^{1}H NMR spectra (discussed immediately below). It thus provides further support for proposed π–π charge transfer interaction between the electron-rich receptor and the electron-deficient analyte and is fully consistent with the proposed charge-transfer-based fluorescence quenching.[19d]

Proton NMR spectroscopic studies were carried out in an effort to obtain insights into the nature of the complex(es)

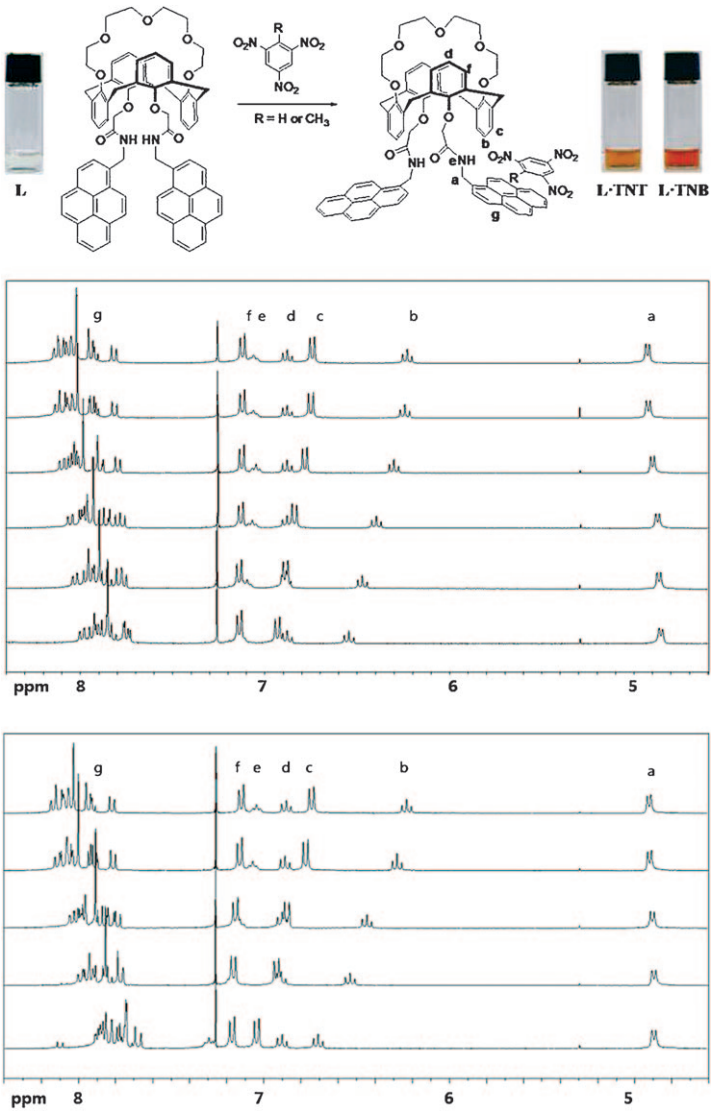

Figure 5. Changes in the ^{1}H NMR spectrum of **L** (5 mM) upon being subject to titration with increasing concentrations of TNT (0, 1, 10, 30, 50, 90 equiv; top) and TNB (0, 1, 5, 10, 30 equiv; bottom) in $CDCl_3$.

formed with **L** as the concentration of TNT or TNB is increased. Towards this end, the ^{1}H NMR spectra of the receptor and putative intermediate species leading to the formation of **L**·TNT and **L**·TNB were recorded in $CDCl_3$. The resulting spectra, reproduced in Figure 5, revealed a gradual shift in the proton resonances for the pyrene, amide, and phenyl groups upon the addition of TNT or TNB. Two proton signals, corresponding to the phenyl (H_b and H_c) and amide groups (H_e), were found to undergo a downfield shift due to the interaction of **L** with the nitro group of TNT as well as the formation of hydrogen-bonds between the nitro and amide groups, respectively. In addition, an upfield shift in the pyrene proton signals was observed; presumably, this reflects the stacking of the pyrene subunit parallel to the nitroaromatic group and the associated ring current effects.

As would be expected, based on the differences in the induced fluorescence quenching response, greater changes in the chemical shifts for **L** were seen upon the addition of TNB than with TNT (for the same number of molar equivalents). We ascribe this difference to electronic effects (TNB is more electron deficient than TNT). However, steric effects cannot be ruled out, since the methyl group of TNT may be too sterically demanding to permit an optimal donor–acceptor interaction as can be inferred from the solid-state structure of **L**·TNT. It was thus expected, as indeed found by experiment, that TNB would be a more effective fluorescence quencher than TNT, and that less electron-deficient species would induce little or no quenching.

To study further the influence of various metal ions on this system, we recorded the fluorescence ratio at 470 nm of **L** (20 μM) in acetonitrile in the presence of 10 molar equivalents of the two nitroaromatics, TNB and TNT, in the presence and absence of 10 molar equivalents of Ag^+, Ba^{2+}, Ca^{2+}, Cd^{2+}, Co^{2+}, Fe^{2+}, Hg^{2+}, K^+, Mg^{2+}, Na^+, Pb^{2+}, Rb^+, and Sr^{2+} with perchlorate counteranions (200 μM). Little effect was seen in the case of most of the cations (cf. Figure S7 and S8 in the Supporting Information). However, the addition of Pb^{2+} to a solution of **L**·X (X = TNT or TNB) remarkably diminished the fluorescence intensities of the pyrene excimer. This finding is currently interpreted in terms of the Pb^{2+} ion being complexed by the two amide groups, something that would serve to quench the excimer signal through reverse PET or a heavy-metal effect.[17b] Further study of this cation specificity is ongoing and a more detailed explanation awaits additional theoretical and experimental analysis.

To provide a firmer theoretical basis for the above empirical findings, density functional theory (DFT) calculations were carried out using the MKWB1K program and the 3-21G* basis set provided by the suite of Gaussian 03 programs.[21] The dipyrenylcalix[4]arene with several potential quenchers were studied in this way in an effort to obtain support for the proposed quenching mechanism. Figure 6 shows the optimized structures of the **L**·X complexes in question. The fluorophore (pyrene) in all complexes shows intermolecular π–π interactions with the selected quencher. Furthermore, in all cases a cofacial, stacked geometry is maintained. For both **L**·benzene and **L**·toluene, the distance between the pyrene molecular plane and that of the quencher was calculated to be almost the same (4.06 Å).

However, in the case of **L**·nitrobenzene, the spacing decreases to 2.94 Å. The distance further decreases to 2.85 Å in **L**·TNT. The calculated spacing is somewhat smaller than the crystal structure; presumably, this reflects the fact that TNT interacts with two molecules of **L** in the crystal structure, which serves to weaken the individual effect. In the event, the differences in donor–acceptor distance are thought to be responsible for, or at least reflect, differences in the charge-transfer quenching features as the result of disparities in the extent of intermolecular coupling between the respective π surfaces. As shown in Figure S9 (in the Supporting Information), the present calculations also revealed

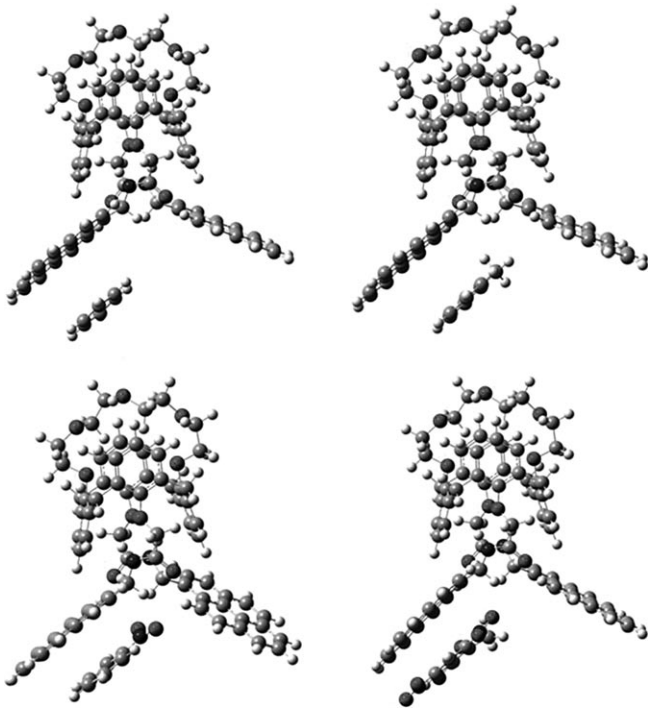

Figure 6. Optimized structure of **L**·X complexes: **L**·benzene (top left); **L**·toluene (top right); **L**·nitrobenzene (bottom left); **L**·TNT (bottom right).

that the LUMO electron distribution of those complexes in which the quencher is decorated with nitro groups is quite different from those not bearing these substituents. On the other hand, in all the complexes created through geometry optimization, the HOMO electrons are found to be on one of the pyrene groups (fluorophore). When excited to the LUMO, some of the electron density is transferred from one pyrene group to another pyrene moity, at least in the case of the presumably weak **L**·benzene and **L**·toluene complexes; this in turn, induces strong electron–hole interactions between the two pyrene moities as reported previously.[17b] In contrast, for **L**·nitrobenzene and **L**·TNT, electron density is transferred from a pyrene subunit to the quencher, a transfer that is clearly expected to account for, or at least contribute substantially, to the observed fluorescence quenching.

Further investigations were performed using TDDFT calculations that have been reported as being useful in understanding the fluorescence behavior of organic molecules.[22] Table 1 lists the dominant electronic oscillators for the strong absorptions based on the corresponding oscillator strengths (OS). For **L**·benzene, the HOMO→LUMO transition has the highest OS value among the selected complexes, and the value for the HOMO−1→LUMO transition is also high (0.2566). The second highest OS value is assigned to the HOMO−1→LUMO transition in **L**·toluene and has a value of 0.2637. For the complexes containing nitro groups, the OS value sharply decreases.

Table 1. Calculated TDDFT excitation properties reflecting the main excitations and oscillator strengths of the various putative complexes **L**·X.

	Excitation	Oscillator strength
L·benzene	HOMO→LUMO	0.4561
	HOMO−1→LUMO	0.2566
L·toluene	HOMO→LUMO	0.0037
	HOMO−1→LUMO	0.2637
L·nitrobenzene	HOMO→LUMO	0.0000
	HOMO−1→LUMO	0.0256
L·TNT	HOMO→LUMO	0.0001
	HOMO−1→LUMO	0.0109

Both HOMO→LUMO transitions for **L**·nitrobenzene and **L**·TNT are very limited. The OS value for the HOMO−1→LUMO transition in **L**·TNT is more than 20 times smaller than that for the corresponding transitions in **L**·benzene and **L**·toluene. Furthermore, the HOMO−1 and LUMO shapes for **L**·nitrobenzene and **L**·TNT are consistent with interactions between electrons present in one pyrene subunit of **L** and the holes in the nitrated aromatics being responsible for the fluorescence quenching. It thus stands to reason, as indeed is seen by experiment, that TNT and TNB are more effective quenchers than the corresponding mononitro species. This has the practical consequence that the highest response is seen for the more explosive members of the series of cannonical nitroaromatic compounds included in the present study.

Conclusion

In summary, we have developed a new and effective fluorescent chemosensor, dipyrenylamidocalix[4]arene–[15]crown-5 (**L**), that allows for the detection of trinitroaromatics species at low concentrations in CH_3CN. When highly nitrated aromatic species, such as TNT and TNB, are added to solutions of **L** in CH_3CN, both the monomer and excimer emissions of the receptor are subject to marked quenching. This is ascribed to a charge-transfer event involving direct interaction between a pyrene subunit and the nitroaromatic analyte. A single-crystal X-ray crystal structure of **L**·TNT provides support for the proposed charge-transfer mechanism in that it reveals a close, stacked interaction between electron donor and quencher in the solid state, a finding that is also supported by TDDFT calculation. To the best of our knowledge, the present dipyrenylcalix[4]arene represents the first pyrene-based system that has been used for the fluorescence-based detection of nitroaromatic species. It is hoped that its efficacy and mode of operation will guide the further development of chemosensors for these and other neutral analytes.

Experimental Section

Details of the sensor synthesis and the spectroscopic measurements can be found in the in the Supporting Information.

CCDC-757957 contains the supplementary crystallographic data for this paper. These data can be obtained free of charge from The Cambridge Crystallographic Data Centre via www.ccdc.cam.ac.uk/data_request/cif.

Acknowledgements

This work was supported by the CRI program of the National Research Foundation of Korea (J.S.K). The work at SKKU was supported by the NRF grants (No. R11-2007-012-03002-0 (2009) and KRF-2008-313-C00388) funded by the Korea Government (MEST). The work in Austin was supported by the U.S. National Science Foundation (grant 0730053 to J.L.S.).

[1] A. M. Rouhi, *Chem. Eng. News* **1997**, *75*, 14–22.
[2] J. I. Steinfeld, J. Wormhoudt, *Annu. Rev. Phys. Chem.* **1998**, *49*, 203–232.
[3] J. V. Goodpaster, V. L. McGuffin, *Anal. Chem.* **2001**, *73*, 2004–2011, and reference therein.
[4] Toxicological profile for 2,4,6-trinitrotoluene, US Department of Health and Human Services, Public Health Service, Agency for Toxic Substances and Disease Registry, **1995**.
[5] a) F. Fant, A. de Sloovere, K. Matthijsen, C. Marle, S. Fantroussi, W. Verstraete, *Environmental Pollution, Vol. 111*, Elsevier, Oxford, **2000**, p. 503; b) Environmental Protection Agency, innovative treatment technologies: Annual status report, 8th ed, **1996**.
[6] J. C. Sanchez, A. G. DiPasquale, A. L. Rheingold, W. C. Trogler, *Chem. Mater.* **2007**, *19*, 6459–6470, and reference therein.
[7] J. Wang, S. B. Hocevar, B. Ogorevc, *Electrochem. Commun.* **2004**, *6*, 176–179.
[8] a) C.-Y. Lai, B. G. Trewyn, D. M. Jeftinija, K. Jeftinija, S. Xu, S. Jeftinija, V. S.-Y. Lin, *J. Am. Chem. Soc.* **2003**, *125*, 4451–4459; b) M. Numata, C. Li, A.-H. Bae, K. Kaneko, K. Sakurai, S. Shinkai, *Chem. Commun.* **2005**, 4655–4657; c) N. Shao, Y. Zhang, S. Cheung, R. Yang, W. Chan, T. Mo, K. Li, F. Liu, *Anal. Chem.* **2005**, *77*, 7294–7303.
[9] H. Sohn, M. J. Sailor, D. Magde, W. C. Trogler, *J. Am. Chem. Soc.* **2003**, *125*, 3821–3830, and reference therein.
[10] a) S. J. Toal, D. Magde, W. C. Trogler, *Chem. Commun.* **2005**, 5465–5467; b) J. C. Sanchez, W. C. Trogler, *J. Mater. Chem.* **2008**, *18*, 3143–3156.
[11] S. W. Thomas, G. D. Joly, T. M. Swager, *Chem. Rev.* **2007**, *107*, 1339–1386.
[12] a) S. Content, W. C. Trogler, M. J. Sailor, *Chem. Eur. J.* **2000**, *6*, 2205–2213; b) M. E. Germain, M. J. Knapp, *Chem. Soc. Rev.* **2009**, *38*, 2543–2555.
[13] M. E. Germain, T. R. Vargo, B. A. McClure, J. J. Rack, P. G. V. Patten, M. Odoi, M. J. Knapp, *Inorg. Chem.* **2008**, *47*, 6203–6211.
[14] a) K. A. Nielsen, W.-S. Cho, J. O. Jeppesen, V. M. Lynch, J. Becher, J. L. Sessler, *J. Am. Chem. Soc.* **2004**, *126*, 16296–16297; b) D. S. Kim, V. M. Lynch, K. A. Nielsen, C. Johnsen, J. O. Jeppesen, J. L. Sessler, *Anal. Bioanal. Chem.* **2009**, *395*, 393–400; c) J. S. Park, F. L. Derf, C. M. Bejger, V. M. Lynch, J. L. Sessler, K. A. Nielsen, C. Johnsen, J. O. Jeppesen, *Chem. Eur. J.* **2010**, *16*, 848–854.
[15] J. S. Kim, D. T. Quang, *Chem. Rev.* **2007**, *107*, 3780–3799, and reference therein.
[16] a) A. P. de Silva, H. Q. N. Gunaratne, T. Gunnlaugsson, A. J. M. Huxley, C. P. McCoy, J. T. Rademacher, T. E. Rice, *Chem. Rev.* **1997**, *97*, 1515–1516; b) F. D. Lewis, Y. Zhang, R. L. Letsinger, *J. Am. Chem. Soc.* **1997**, *119*, 545–5452.
[17] a) F. M. Winnik, *Chem. Rev.* **1993**, *93*, 587–614; b) S. K. Kim, S. H. Lee, J. Y. Lee, R. A. Bartsch, J. S. Kim, *J. Am. Chem. Soc.* **2004**, *126*, 16499–16506; c) H. N. Kim, M. H. Lee, H. J. Kim, J. S. Kim, J. Yoon, *Chem. Soc. Rev.* **2008**, *37*, 1465.
[18] C. J. Broan, *Chem. Commun.* **1996**, 699–700.
[19] a) K. S. Washburn, K. C. Donnelly, H. J. Huebner, R. C. Burghardt, T. C. Sewall, L. D. Claxton, *Chemosphere* **2001**, *44*, 1703–1709;

b) H. Bai, C. Li, G. Shi, *Sens. Actuators B* **2008**, *130*, 777–782; c) S. Zhang, F. Lü, L. Ding, Y. Fang, *Langmuir* **2007**, *23*, 1584–1590; d) S. Burattini, H. M. Colquhoun, B. W. Greenland, W. Hayes, M. Wade, *Macromol. Rapid Commun.* **2009**, *30*, 459–463.

[20] P. J. Suppan, *J. Chem. Soc. Faraday Trans. 1* **1986**, *82*, 509–511.

[21] Gaussian 03, Revision C.02, M. J. Frisch, G. W. Trucks, H. B. Schlegel, G. E. Scuseria, M. A. Robb, J. R. Cheeseman, J. A. Montgomery, Jr., T. Vreven, K. N. Kudin, J. C. Burant, J. M. Millam, S. S. Iyengar, J. Tomasi, V. Barone, B. Mennucci, M. Cossi, G. Scalmani, N. Rega, G. A. Petersson, H. Nakatsuji, M. Hada, M. Ehara, K. Toyota, R. Fukuda, J. Hasegawa, M. Ishida, T. Nakajima, Y. Honda, O. Kitao, H. Nakai, M. Klene, X. Li, J. E. Knox, H. P. Hratchian, J. B. Cross, V. Bakken, C. Adamo, J. Jaramillo, R. Gomperts, R. E. Stratmann, O. Yazyev, A. J. Austin, R. Cammi, C. Pomelli, J. W. Ochterski, P. Y. Ayala, K. Morokuma, G. A. Voth, P. Salvador, J. J. Dannenberg, V. G. Zakrzewski, S. Dapprich, A. D. Daniels, M. C. Strain, O. Farkas, D. K. Malick, A. D. Rabuck, K. Raghavachari, J. B. Foresman, J. V. Ortiz, Q. Cui, A. G. Baboul, S. Clifford, J. Cioslowski, B. B. Stefanov, G. Liu, A. Liashenko, P. Piskorz, I. Komaromi, R. L. Martin, D. J. Fox, T. Keith, M. A. Al-Laham, C. Y. Peng, A. Nanayakkara, M. Challacombe, P. M. W. Gill, B. Johnson, W. Chen, M. W. Wong, C. Gonzalez, J. A. Pople, Gaussian, Inc., Wallingford CT, **2004**.

[22] a) H. J. Kim, S. Bhuniya, R. K. Mahajan, R. Puri, H. Liu, K. C. Ko, J. Y. Lee, J. S. Kim, *Chem. Commun.* **2009**, 7128–7130; b) H. S. Jung, P. S. Kwon, J. W. Lee, J. I. Kim, C. S. Hong, J. W. Kim, S. Yan, J. Y. Lee, J. H. Lee, T. Joo, J. S. Kim, *J. Am. Chem. Soc.* **2009**, *131*, 2008–2012; c) H. J. Kim, S. K. Kim, J. Y. Lee, J. S. Kim, *J. Org. Chem.* **2006**, *71*, 6611–6614; d) S. K. Kim, J. H. Bok, R. A. Bartsch, J. Y. Lee, J. S. Kim, *Org. Lett.* **2005**, *7*, 4839–4842; e) D. Ryu, E. Park, D.-S. Kim, S. Yan, J. Y. Lee, B.-Y. Chang, K. H. Ahn, *J. Am. Chem. Soc.* **2008**, *130*, 2394–2395.

Received: December 15, 2009
Published online: April 29, 2010

